

Petrophysical Evaluation of FUBA Field Reservoir in Onshore Niger Delta, Nigeria, Using 3-D Seismic and Well Logs

U. Ochoma^{1*}

¹Department of Physics, Rivers State University, P.M.B 5080, Port Harcourt, Nigeria.
Corresponding Author Email: umaocho@gmail.com*



DOI: <https://doi.org/10.46382/MJBAS.2024.8109>

Copyright: © 2024 U. Ochoma. This is an open-access article distributed under the terms of the Creative Commons Attribution License, which permits unrestricted use, distribution, and reproduction in any medium, provided the original author and source are credited.

Article Received: 18 December 2023

Article Accepted: 25 February 2024

Article Published: 29 March 2024

ABSTRACT

Petrophysical evaluation of Fuba Field reservoir in Onshore Niger Delta, Nigeria, are here presented, using 3-D Seismic and Well Logs. Well-to-seismic ties, faults mapping, horizon mapping, petrophysical evaluation and petrophysical attributes maps generation were carried out using Petrel software. The structural interpretation of seismic data reveals highly synthetic and antithetic faults which are in line with faults trends identified in the Niger Delta. These faults play significant roles in trap formation at the upper, middle and lower sections of the field. Three distinct horizons were mapped. Reservoir M is found at a shallower depth from 10937 to 10997 ft, reservoir N is found at a depth ranging from 11213 to 11241 ft while reservoir O is found at a deeper depth ranging from 11681 to 11871 ft respectively. The well logs suite contained the following logs: Gamma ray; Deep Resistivity; Density; Sonic and Neutron. Petrophysical properties evaluated are; thickness, porosity, permeability, water saturation and net-to-gross. From the result, on average, net thickness, effective porosity, permeability, net to gross (NTG) and water saturation values are 58.00 ft, 20.30%, 1022.53 mD, 65% and 38% for reservoir sand M, 28.00 ft, 19.30%, 602.57 mD, 27.00% and 48.00% for reservoir sand N and 169.71 ft, 20.14%, 1224.00 mD, 68% and 37% for reservoir sand O. The high values of porosity and permeability have been classed as good to excellent for reservoir sand M and O respectively and suggest higher proportion of sand than shale within the reservoir sand units. An analysis of the petrophysical attributes maps shows that well-4 has the best petrophysical qualities on reservoir sand M while well-2 and well-3 have the best petrophysical qualities on reservoir sand O. The results for this study can be used for well drilling and petroleum production programmes in the study area.

Keywords: Petrophysical properties; Water saturation; Porosity; Permeability; Niger Delta; Nigeria.

1.0. Introduction

A reservoir is one which by virtue of its porosity and permeability is capable of containing a reasonable quantity of hydrocarbon if entrapment conditions are right, but can also release hydrocarbon at a satisfactory rate when the reservoir is penetrated by a well (Etu-Efeotor, 1997). Reservoir quality analysis is aimed at identifying hydrocarbon bearing reservoirs, delineating them and subsequently, determining the distribution of relevant physical properties such as lithology, porosity, permeability, water saturation and pore pressure, which will make for an easy determination of the reservoir's economic potential (Nwajide, 2013). Defining petrophysical properties such as permeability, fluid saturation, areal extent, thickness of reservoir and porosity is very vital to the oil and gas industry (Saadu and Nwankwo, 2008). A homogenous reservoir might have some of these properties constant whereas they might vary significantly in a heterogeneous reservoir, as is the case with reservoir rocks in the Niger Delta (Tiab and Donaldson, 2004). These parameters when combined with geologic and petrophysical data give a complete picture of the reservoir (Tamunosiki et al., 2014).

Many literatures have reported interesting petrophysical evaluation studies in the oil prolific area of the Niger Delta Basin, Nigeria (Omoboriowo et al., 2012; Osinowo et al., 2017; Eshimokhai and Akhirevbulu, 2012; Adizua and Oruade, 2018). Omoboriowo et al., (2012) evaluated the reservoir characterization of KONGA field, onshore Niger Delta, Nigeria using a suite of wireline logs from five wells and biofacies data was taken. The results show that the rock properties are variable and are controlled by environments of deposition during Oligocene – late Miocene. Osinowo et al., (2017) generated reservoir structural framework and spatial reservoir

property distribution have proved useful to guide the optimal placement of wells and also provide information needful for the development of best production plan that would guarantee effective oil drainage from the delineated reservoirs.

This study is taken from Fuba Field, Onshore, Niger Delta, Nigeria. The ultimate deliverable of this study was petrophysical evaluation of reservoir sands using 3D seismic and well logs of the area. The major components of the study are: (a) Petrophysical evaluation. (b) Well Correlation performed in order to determine the continuity of the reservoir sand across the field. (c) Seismic Interpretation which involves well-to-seismic tie, fault mapping and horizon mapping. This aids in giving more insight into petrophysical evaluation of reservoir sands using 3D seismic and well logs.

2.0. Location and Geology of the Study Area

The proposed study area Fuba Field is located in the onshore Niger Delta region. Figure 1 shows the map of the Niger Delta region showing the location of the study area while Figure 2 shows the base map showing well locations in the study area. The Niger Delta lies between latitudes 4° N and 6° N and longitudes 3° E and 9° E (Whiteman, 1982). The Delta ranks as one of the major oil and gas provinces globally, with an estimated ultimate recovery of 40 billion barrels of oil and 40 trillion cubic feet of gas (Adegoke et al., 2017). The coastal sedimentary basin of Nigeria has been the scene of three depositional cycles (Short and Stauble, 1967). The first began with a marine incursion in the middle Cretaceous and was terminated by a mild folding phase in Santonian time. The second included the growth of a proto-Niger delta during the Late Cretaceous and ended in a major Paleocene marine transgression. The third cycle, from Eocene to Recent, marked the continuous growth of the main Niger delta. A new threefold lithostratigraphic subdivision is introduced for the Niger delta subsurface, comprising an upper sandy Benin Formation, an intervening unit of alternating sandstone and shale named the Agbada Formation, and a lower shaly Akata Formation. These three units extend across the whole delta and each ranges in age from early Tertiary to Recent. They are related to the present outcrops and environments of deposition.

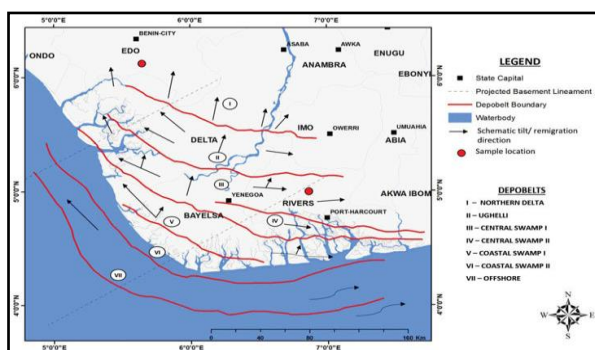


Figure 1. Map of Niger Delta Showing the study Area

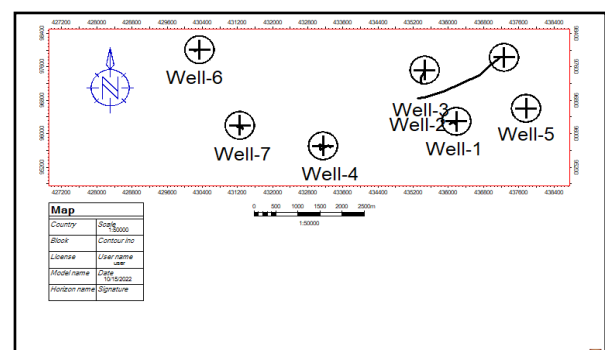


Figure 2. Base Map Showing Well Locations in the Study Area

A separate member of the Benin Formation is recognized in the Port Harcourt area. It is Miocene-Recent in age with a minimum thickness of more than 6,000ft (1829m) and made up of continental sands and sandstones

(>90%) with few shale intercalations (Horsfall et al., 2017). Subsurface structures are described as resulting from movement under the influence of gravity and their distribution is related to growth stages of the delta (Ochoma et al., 2020). Rollover anticlines in front of growth faults form the main objectives of oil exploration, the hydrocarbons being found in sandstone reservoirs of the Agbada Formation. The oil in geological structures in the basin may be trapped in dip closures or against a synthetic or antithetic fault.

3.0. Materials and Methods

This study makes use of wire line log as well as 3D seismic data. The well log data comprise of a suite of logs; gamma ray, neutron, density, deep resistivity and sonic logs for seven wells. These were key in establishing the reservoir distribution and lateral continuity of the reservoirs in the study area. The interactive Petrel software was used for the study.

3.1. Well-Log and Seismic Data Quality Control

Well correlation involves lithologic description, picking top and base of sand-bodies, fluid discrimination and then linking these properties from one well to another based on similarity in trends. Correlation of reservoir sands was achieved using the top and base of reservoir sands picked. The correlation process was possible based on similarity in the behaviour of the gamma ray log. In the Niger Delta, the predominant lithologies are sands and shales. In order to discriminate between these two lithologies in the subsurface, the gamma ray log is used. The gamma ray log reflects the shale content of sedimentary formations. Clean sandstones and carbonates normally exhibit a low level of natural radioactivity, while clay minerals and fluid particles in shales show higher levels of radioactivity due to adsorption of the heavy radioactive elements (Tiab, and Donaldson, 2004). After defining the lithologies, the resistivity log was used for discriminating the type of fluid occurring within the pores in the rocks. The resistivity log can easily differentiate water from oil because water is conductive and oil is resistant to flow of electrical current. Hence, on the resistivity log, a sharp increase (a kick) in the resistivity measurement indicates the presence of hydrocarbons. The neutron and density cross-over (balloon effect) is often used to differentiate oil from gas in a reservoir. There was no gas present in any of the reservoir sands.

There are four basic steps involved in seismic interpretation relevant to this study and they include; Well-to-seismic ties, Fault Mapping, Horizon mapping and Petrophysical evaluation. Well-to-seismic tie is a process that enables the visualization of well information on seismic data. For this process to be achieved, the following are basic requirements; checkshot, sonic log, density log and a wavelet. The sonic log, which is the reciprocal of velocity, was calibrated using the checkshot data. The calibration process is necessary in order to improve the quality of the sonic log because the sonic log is prone to washouts and other wellbore related issues. The results of calibrating the sonic log with the checkshot gives a new log called the calibrated sonic log.

The calibrated sonic log is used along with the density log to generate an acoustic impedance (AI) log. The acoustic impedance log is calculated for each layer of rock. The next step involves generating the reflectivity coefficient (RC) log. The RC is calculated and generated using the AI log. The RC log generated is then convolved with a wavelet to generate a synthetic seismogram which is comparable with the seismic data. The

extended white 2 wavelet utilized for convolution is extracted from the seismic data. The synthetic seismogram was generated for every well that had checkshot, density and sonic log. The reflections on the synthetic seismogram were matched with the reflections on seismic data. The mathematical expressions that govern the entire well-to-seismic tie workflow are presented below:

$$AI = \rho v \quad (1)$$

$$RC = \frac{\rho_2 v_2 - \rho_1 v_1}{\rho_2 v_2 + \rho_1 v_1} \quad (2)$$

$$\text{Synthetic Seismogram} = \frac{\rho_2 v_2 - \rho_1 v_1}{\rho_2 v_2 + \rho_1 v_1} * \text{wavelet} \quad (3)$$

where AI = acoustic impedance, RC = reflection coefficient, ρ = density; v = velocity.

Faults were identified as discontinuities or breaks in the seismic reflections. Faults were mapped on both inline and cross-line directions. Horizons are continuous lateral reflection events that are truncated by fault lines. The horizon interpretation process was conducted along both inline and crossline direction.

3.2. Petrophysical Evaluation

Four main petrophysical parameters are important in defining any reservoir, which include: effective porosity (ϕ_E), Net to Gross (NTG), permeability (K) and water saturation (S_w). Various equations applicable to the Niger Delta were utilized for their computation in this study.

3.2.1. Effective Porosity

The effective porosity is the porosity that is responsible for flow to occur within the reservoir. Effective porosity (ϕ_E) was calculated using volume of shale (V_{sh}) and total porosity (ϕ_T) as follows (Dresser, 1979);

$$\phi_E = (1 - V_{sh}) \times \phi_T \quad (4)$$

Where; ϕ_E = Effective porosity, ϕ_T = Total Porosity, V_{sh} = Volume of shale

3.2.2. Permeability

$$K = v \frac{\mu \Delta x}{\Delta P} \quad (5)$$

Where; K = permeability, v = fluid velocity, μ = dynamic viscosity, Δx = thickness of the bed of the porous medium and ΔP = applied pressure difference.

3.2.3. Net to Gross

The net-to-gross ratio reduces the maximum reservoir thickness to the anticipated pay (permeable reservoir) thickness. Net-to-Gross sand is reservoir thickness less shale thickness (Cannon, 2018). This is a factor used to identify probable producing regions of a formation. To determine the clean sand content, Net to Gross was calculated as follows;

$$Net - to - gross = \frac{NH}{GH} \quad (6)$$

Where;

NH = Net thickness

GH = Gross thickness

3.2.4. Water Saturation

This is the relative extent to which the pores in rocks are filled with water. Saturation is expressed as the fraction, or percent, of the total pore volume occupied by the oil, gas, or water. Water saturation is denoted as S_w and is expressed in percent or fraction. Water saturation is predominantly controlled by porosity and formation resistivity. It can be calculated using Archie's (1942) empirical model as follows;

$$S_w = \left(\frac{a \times R_w}{R_t \times \phi_t^m} \right)^{1/n} \quad (7)$$

Where;

S_w = Archie's water saturation for clean sand

a = tortuosity factor = 1

m = cementation exponent = 2

n = saturation exponent = 2

R_t = formation resistivity (read from log)

R_w = formation water resistivity (read from log)

ϕ_t = total porosity

3.2.5. Petrophysical Attribute Maps

Petrophysical attribute maps are seismic models which can be used to validate the static reservoir models. It is a 2D map view which serves as a model for doing quality check on the 3D petrophysical models. To generate the maps, the average petrophysical parameters are used as input. Petrophysical attributes maps were generated for the horizons of interest.

4.0. Results and Discussion

4.1. Reservoir Identification and Correlation

The results for lithology and reservoir identification are presented in (Figure 3). A total of four sand bodies (L, M, N and O) were identified and correlated across all seven wells in the field. Two reservoir sands were selected for the purpose of this study (M and O). The resistivity logs which reveals the presence of hydrocarbons were used to identify the hydrocarbon bearing sands. On (Figure 3), the sands are coloured yellow while shales are grey in colour.

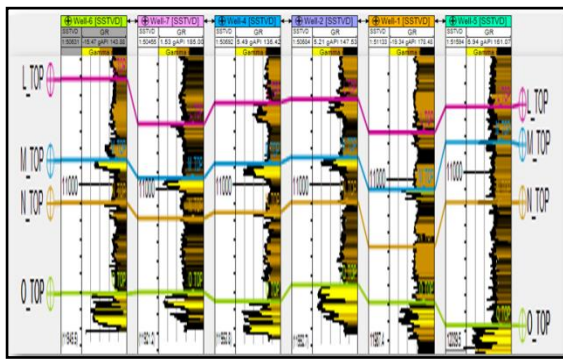


Figure 3. Well section showing reservoir identified and correlated across Fuba Field

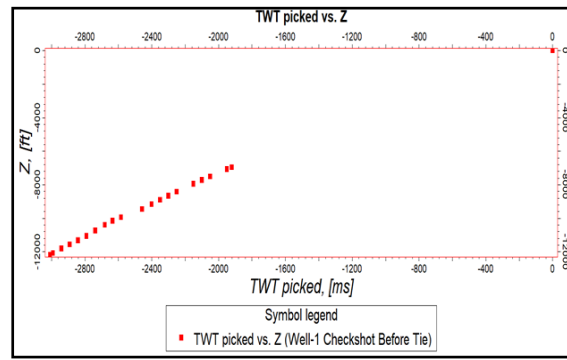


Figure 4. Checkshot Quality check for Well-1

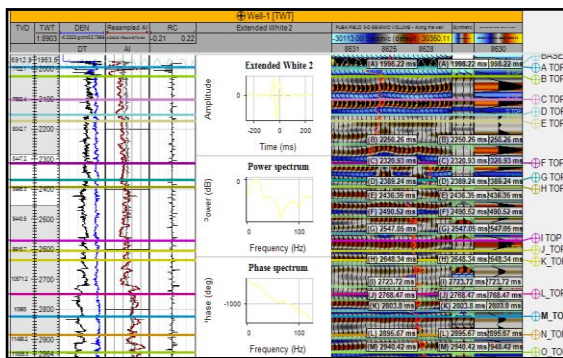


Figure 5. Synthetic seismogram generation and well-to-seismic tie conducted for Fuba Field using Well-1 Checkshot

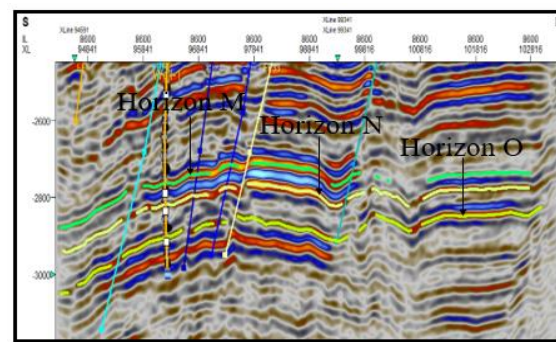


Figure 6. Faults and horizons interpreted along seismic inline section

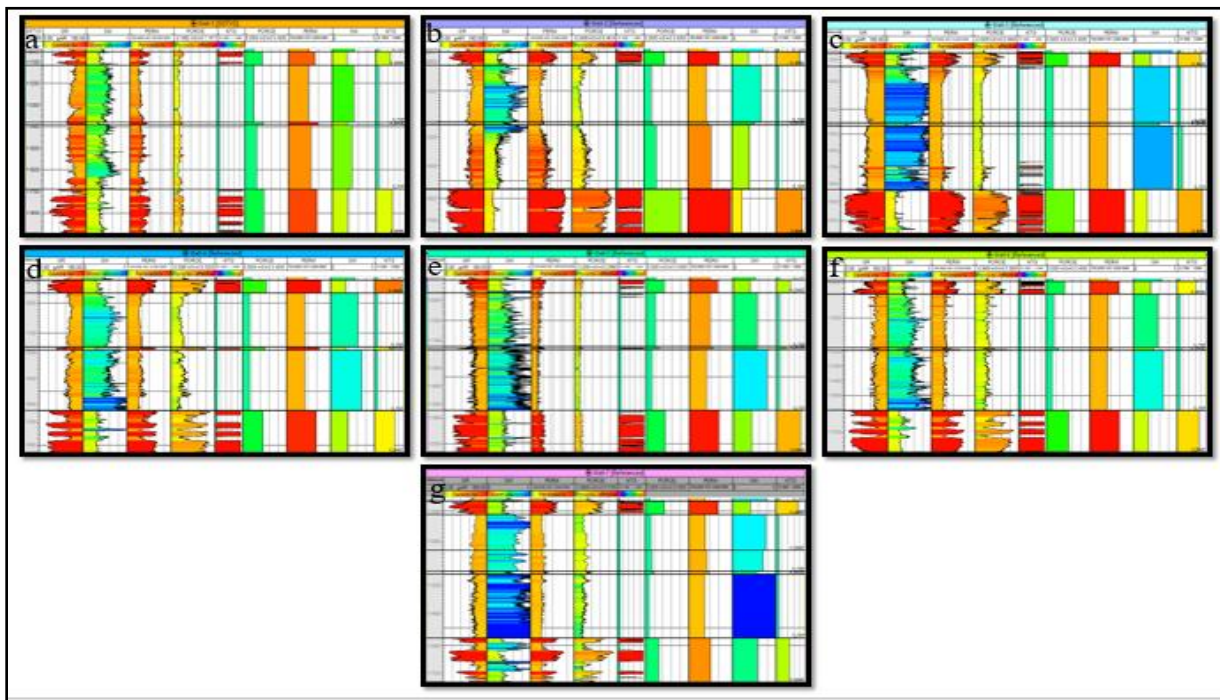


Figure 7. Well-section Showing Petrophysical Attribute Logs and their Respective Averages for wells 1-7 (a-g)

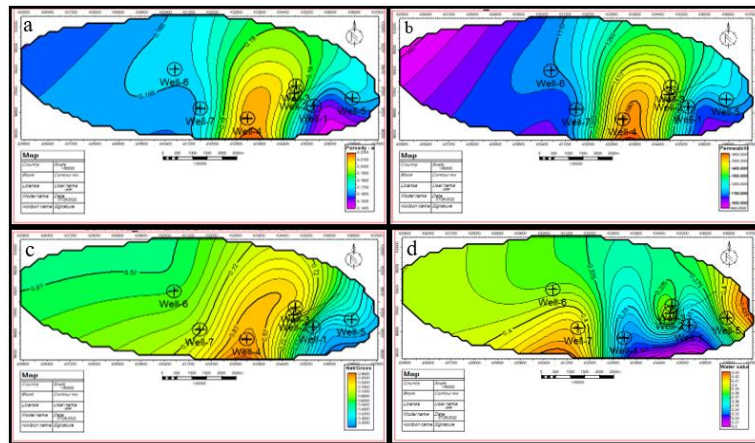


Figure 8. Average Attribute Maps for Reservoir Surface-M: (a) Average Permeability Attribute Map
(b) Average NTG Attribute Map (c) Average Water Saturation Attribute Map
(d) Average Porosity Attribute Map

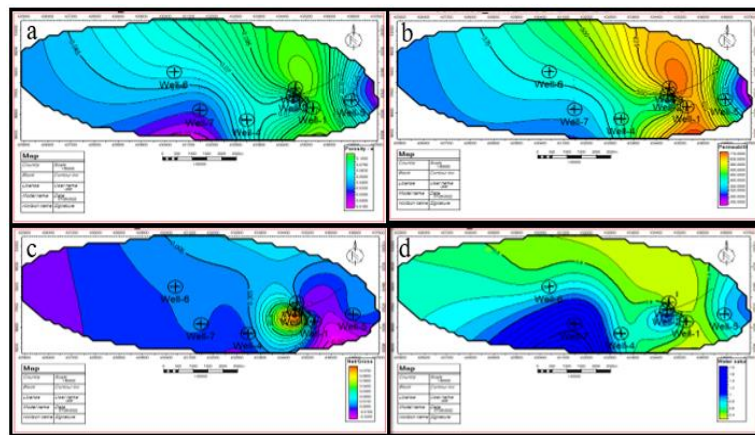


Figure 9. Average Attribute Maps for Reservoir Surface-N: (a) Average Porosity Attribute Map
(b) Average Permeability Attribute Map (c) Average NTG Attribute Map
(d) Average Water Saturation Attribute Map

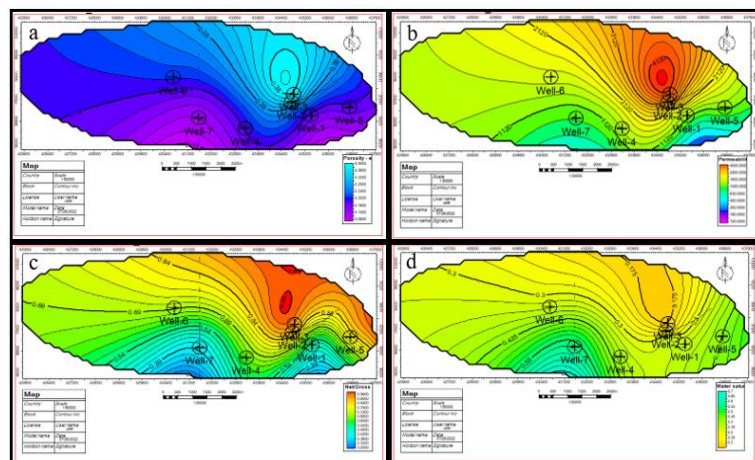


Figure 10. Average Attribute Maps for Reservoir Surface-O (a) Average Porosity Attribute Map
(b) Average Permeability Attribute Map (c) Average NTG Attribute Map
(d) Average Water Saturation Attribute Map

4.2. Well-to-seismic Tie

The checkshot quality check for Well-1 utilized for well-to-seismic tie is shown in Figure 4. The results for well-to-seismic tie conducted on Fuba field using density log, sonic log and checkshot of Well-1 is presented in Figure 5. An extended white 2 wavelet was used to give a near perfect match between the seismic and synthetic seismogram.

4.3. Fault and Horizon Interpretation

The results for the interpreted faults in Fuba field are presented in Figure 6 shows both synthetic and antithetic faults interpreted along seismic inlines. Faults are more visible along the inline direction because this direction reveals the true dip position of geologic structures. The variance time slice was used to validate the interpreted faults. All interpreted faults are normal synthetic and antithetic faults. A total of thirty-six faults were interpreted across the entire seismic data. Of the 36 interpreted faults, only F1 (synthetic fault) and F4 (antithetic fault) faults are regional, running from the top to bottom across the field. Hence, these faults play significant roles in trap formation at the upper, middle and lower sections of the field. The results for the interpreted seismic horizons (Horizons M, N and O) are also presented in Figure 6.

4.4. Petrophysical Evaluation

The results of petrophysical evaluation are presented in Figures 7-10 and Tables 1-3. Figure 7 is the well-section showing petrophysical attribute logs and their respective averages for wells 1-7 (a-g). Figure 8-10 show average attribute maps for reservoir surfaces M, N and O. The petrophysical properties include net thickness, effective porosity, permeability, net to gross and water saturation.

4.4.1. Net Thickness

The reservoir net thickness which is the clean sand portion of the reservoir ranges from 10.00 to 87.00 ft in reservoir sand M (Table 1), 14.00 to 77.00 ft reservoir sand N (Table 2) and 159.00 to 229.00 ft in reservoir sand O (Table 3). In reservoir sand M, well-4 showed the highest net thickness, while the least net thickness was found in well-5. In reservoir sand N, well-3 showed the highest net thickness, while the least net thickness was found in well-1 and well-5. Also, in reservoir sand O, well-3 showed the highest net thickness, while the least net thickness was found in well-5. On the average, net sand thickness is 58.00 ft, 28.00 ft and 169.71 ft in reservoir sands M, N and O respectively. These results show that sufficient thickness of the reservoirs M and O are available as net sands (clean producible sand, provided they contain hydrocarbons) while reservoir N is a thin sand.

4.4.2. Effective Porosity

Effective porosity ranged from 18.00 to 23.00%, 17.00 to 20.00% and 12.00 to 27.00% in reservoir sand M, N and reservoir sand O respectively. In reservoir sand M, well-3 and well-4 showed the highest effective porosities, while the least effective porosity was found in well-1 (Figure 8a). In reservoir sand N, well-3 showed the highest effective porosity, while the least effective porosity was found in well-1 (Figure 9a). In reservoir sand O, well-2 and well-3 showed the highest effective porosity, while the least effective porosity was found in well-7 (Figure

10a). On average, effective porosity is 20.30%, 19.30% and 20.14% in reservoir sands M, N and O respectively. There is a decreasing trend of porosity from reservoir sand M to reservoir sand O. The porosity that is responsible for flow and accumulation in a reservoir is the effective porosity. Rocks have negligible porosity when $< 5\%$, poor porosity when $>5-10\%$, good porosity when $>10-20\%$, very good when $>20-30\%$, and excellent when $>30\%$ (Levorsen, 1967). Based on this classification scheme, the average effective porosity for the reservoirs (M, N and O) are classed as very good. These results suggest that the reservoirs are porous enough to allow for accumulation of hydrocarbons.

4.4.3. Permeability

The results of reservoir permeability ranges from 768.60 to 1412.00 mD in reservoir sand M (Table 1), 455.60 to 1196.60 mD in reservoir sand N (Table 2) and 552.80 to 2618.70 mD in reservoir sand O (Table 3). In reservoir sand M well-4 showed the highest permeability, while the least permeability was found in well-1 (Figure 8b). In reservoir sand N well-2 showed the highest permeability, while the least permeability was found in well-7 (Figure 9b). In reservoir sand O, well-2 showed the highest permeability, while the least permeability was found in well-7 (Figure 10b). The average permeability values recorded in reservoir sands M, N and O are 1022.53 mD, 602.57 mD and 1224.00 mD. On average, permeability in the three reservoirs are greater than 250 mD. Rider, (1996) classified reservoir quality based on permeability values are as follows; < 10 mD (poor to fair), $>10-50$ mD (moderate), $>50-250$ mD (Good), $>250-1000$ mD (very good) and >1000 mD (excellent). Based on this classification scheme, reservoir sand M, N and O are classed as having very good quality. These values are typical of Niger Delta reservoirs. Hence, fluid flow within these reservoir units will occur with ease because of the relatively high permeability values.

4.4.4. Net to Gross

The net to gross ratio ranges from 41 to 91% in reservoir sand M (Table 1), 23 to 55% in reservoir sand N (Table 2) and 41 to 87% in reservoir sand O (Table 3) respectively. In reservoir sand M, well-4 showed the highest net to gross, while the least net to gross ratio was found in well-5 (Figure 8c). In reservoir sand N, well-2 showed the highest net to gross, while the least net to gross ratio was found in well-7 (Figure 9c). In reservoir sand O, well-2 showed the highest net to gross, while the least net to gross ratio was found in well-7 (Figure 10c). On average, net to gross ratio are 65%, 27% and 68% in reservoir sands M, N and O. These results show that both reservoir sands M and O have greater than 60% clean sand volumes, indicating that reservoirs M and O are clean enough for hydrocarbon production, provided they are hydrocarbon bearing while reservoir sand N is a thin sand with thin pay zone.

4.4.5. Fluid Saturation

Water saturation ranged from 34 to 41% in reservoir sand M (Table 1), 32 to 60% in reservoir sand N (Table 2) and 22 to 57% in reservoir sand O (Table 3). In reservoir sand M, well-7 showed the highest water saturation, while the lowest water saturation was found in well-1 and well-4 (Figure 8d). In reservoir sand N, well-7 showed the highest water saturation, while the lowest water saturation was found in well-1 (Figure 9d). In reservoir sand

O, well-7 showed the highest water saturation, while the lowest water saturation was found in well- 2 and well-3 (Figure 10d). On average, the water saturations in the hydrocarbon reservoirs are 38.00, 48.00 and 37.00% for reservoir sands M, N and O respectively. This leads to a corresponding hydrocarbon saturation of 62.00, 52.00 and 63.00% in reservoir sand M and O respectively. Based on these results, reservoir sand O has the highest hydrocarbon saturation while reservoir sand N has the least. These hydrocarbon saturation values are good for reservoir development for production.

Table 1. Results of Petrophysical Evaluation for Reservoir Surface M

Wells	Net thickness (ft)	Effective Porosity (%)	Permeability (mD)	NTG (%)	Water Saturation (%)
Well-1	45.00	18.00	768.60	45.00	34.00
Well-2	48.00	21.00	1095.00	76.00	36.00
Well-3	76.00	23.00	1098.00	73.00	39.00
Well-4	87.00	23.00	1412.00	91.00	34.00
Well-5	10.00	19.00	893.80	41.00	40.00
Well-6	58.00	19.00	950.10	60.00	39.00
Well-7	82.00	19.00	941.00	70.00	41.00
Average	58.00	20.30	1022.53	65.00	38.00

Table 2. Results of Petrophysical Evaluation for Reservoir Surface N

Wells	Net thickness (ft)	Effective Porosity (%)	Permeability (mD)	NTG (%)	Water Saturation (%)
Well-1	14.00	17.00	974.60	0.00	33.00
Well-2	16.00	20.00	1196.60	55.00	51.00
Well-3	77.00	22.00	448.30	0.00	58.00
Well-4	28.00	20.00	448.00	0.00	32.00
Well-5	14.00	18.00	600.00	23.00	54.00
Well-6	26.00	18.00	542.90	3.00	45.00
Well-7	18.00	18.00	455.60	0.00	60.00
Average	28.00	19.30	602.57	27.00	48.00

Table 3. Results of Petrophysical Evaluation for Reservoir Surface O

Wells	Net thickness (ft)	Effective Porosity (%)	Permeability (mD)	NTG (%)	Water Saturation (%)
Well-1	209.00	17.00	881.20	51.00	35.00
Well-2	203.00	30.00	2618.70	87.00	22.00
Well-3	229.00	27.00	1574.80	81.00	31.00
Well-4	183.00	19.00	953.00	63.00	38.00
Well-5	159.00	18.00	982.40	80.00	43.00
Well-6	186.00	18.00	1004.00	70.00	34.00
Well-7	162.00	12.00	552.80	41.00	57.00
Average	169.71	20.14	1224.00	68.00	37.00

5.0. Conclusion

The structural interpretation of seismic data reveal highly synthetic and antithetic faults which are in line with faults trends identified in the Niger Delta. Of the 36 interpreted faults, only synthetic and antithetic faults are regional, running from the top to bottom across the field. These faults play significant roles in trap formation at the upper, middle and lower sections of the field. Three distinct horizons were mapped. Reservoir M is found at a shallower depth from 10937 to 10997 ft, reservoir N is found at a depth ranging from 11213 to 11241 ft while reservoir O is found at a deeper depth ranging from 11681 to 11871 ft respectively. The three hydrocarbon reservoirs showed lateral continuity across the wells and fall within the Agbada formation where most of the hydrocarbon is believed to be trapped. Petrophysical properties evaluated are; thickness, porosity, permeability, water saturation and net-to-gross. The well logs suite contained the following logs: Gamma ray; Deep Resistivity; Density; Sonic and Neutron. From the result, on average, net thickness, effective porosity, permeability, net to gross (NTG) and water saturation values are 58.00 ft, 20.30%, 1022.53 mD, 65% and 38% for reservoir sand M, 28.00 ft, 19.30%, 602.57 mD, 27.00% and 48.00% for reservoir sand N and 169.71 ft, 20.14%, 1224.00 mD, 68% and 37% for reservoir sand O. The high values of porosity and permeability have been classed as good to excellent for reservoir sands M, N and O respectively and suggest higher proportion of sand than shale within the reservoir sand units. This is typical of clastic reservoir systems in the Niger Delta. The results show that the hydrocarbon bearing zones of the reservoirs are highly porous and highly permeable. The results for water saturation are good and favourable for hydrocarbon production while the results for NTG show that the reservoir rocks are predominantly composed of clean sands. An analysis of the petrophysical attributes maps shows that well-4 has the best petrophysical qualities on reservoir sand M while well-2 and well-3 have the best petrophysical qualities on reservoir sand O due to the low values of water saturation and high values of permeability, porosity and NTG.

This is based on well placement in the study area. Hydrocarbon volume estimation should be done on the studied reservoirs to ascertain the volume of hydrocarbon in them. The results for this work can be used for well drilling and petroleum production programmes in the study area.

Declarations

Source of Funding

This study did not receive any grant from funding agencies in the public, commercial, or not-for-profit sectors.

Competing Interests Statement

The author declares no competing financial, professional, or personal interests.

Consent for publication

The author declares that she consented to the publication of this study.

Acknowledgements

The author is grateful to Shell Petroleum Development Company of Nigeria (SPDC), Port Harcourt Nigeria for the release of the academic data for the purpose of this study.

References

- [1] Etu-Efeotor, J.O. (1997). *Fundamentals of Petroleum Geology*. Paragraphics: Port Harcourt, PH.
- [2] Nwajide, C.S. (2013). *Geology of Nigeria's Sedimentary Basins*. CSS Bookshops Limited, Lagos.
- [3] Saadu, K.Y., & Nwankwo, N.C. (2008). Petrophysical Evaluation and Volumetric Estimation within Coastal Swamp Depobelt, Niger Delta, Using 3-D Seismic and Well Logs. *Egyptian Journal of Petroleum*, 27: 531–539.
- [4] Tiab, D., & Donaldson, E.C. (2004). *Petrophysics: Theory and Practice of Measuring Reservoir Rock and Fluid Transport*, 2nd edition. 2001 Gulf Professional Publishing, U.S.A.
- [5] Tamunosiki, D., Ming, H.G., Wang, L., Uko, E.D., & Tamunonengiyeofori, W. (2014). Petrophysical Characteristics of Coastal Swamp Depobelt Reservoir in the Niger Delta Using Well-Log Data. *IOSR Journal of Applied Geology and Geophysics*, 2(2): 76–85.
- [6] Omoboriowo, A.O., Chiaghanam, O.I., Chiadikobi, K.C., Oluwajana, O.A., Soronnadi-Ononiwu, C.G., & Ideozu, R.U. (2012). Reservoir Characterization of KONGA Field, Onshore Niger Delta, Southern Nigeria. *International Journal of Science and Emerging Technology*, 3(1): 19–30.
- [7] Osinowo, O.O., Ayorinde, O.J., Nwankwo, P.C., Ekeng, O.M., & Taiwo, O.B. (2017). Reservoir Description and Characterization of Eni Field Offshore Niger Delta, Southern Nigeria. *Ozean Journal of Petroleum Exploration Production Technology*, 8(55): 1–17.
- [8] Eshimokhai, S., & Akhirevbulu, O.E. (2012). Reservoir Characterization Using Seismic and Well Logs Data (A Case Study of Niger Delta). *Ethiopian Journal of Environmental studies and Management*, 5(4): 597–603.

- [9] Adizua, O.F., & Oruade, L. (2018). Reservoir Characterization of an offshore Niger Delta “X” Field Using Well Log Data. *International Journal of Engineering, Applied Science and Technology*, 2(12): 1–4.
- [10] Whiteman, A. (1982). *Nigeria: Its Petroleum Ecology Resources and Potential*. London, Graham and Trotman.
- [11] Adegoke, O.S., Oyebamiji, A.S., Edet, J.J., Osterloff, P.L., & Ulu, O.K. (2017). *Cenozoic Foraminifera and Calcareous Nannofossil Biostratigraphy of the Niger Delta*. Elsevier, Cathleen Sether, United States.
- [12] Short, K.C., & Stable A.J. (1967). Outline of Geology of Niger Delta. *Bulletin of America Association of Petroleum Geologists*, 51(5): 761–779.
- [13] Horsfall, O.I., Uko, E.D., Tamunoberetonari I., & Omubo-Pepple, V.B. (2017). Rock-Physics and Seismic-Inversion Based Reservoir Characterization of AKOS FIELD, Coastal Swamp Depobelt, Niger Delta, Nigeria. *IOSR Journal of Applied Geology and Geophysics*, 5(4): 59–67.
- [14] Ochoma, U., Uko E.D., & Horsfall, O.I. (2020). Deterministic Hydrocarbon Volume Estimation of the Onshore Fuba Field, Niger Delta, Nigeria. *IOSR Journal of Applied Geology and Geophysics*, 8(1): 34–40.
- [15] Tiab, D., & Donaldson, E.C. (2004). *Petrophysics: Theory and Practice of Measuring Reservoir Rock and Fluid Transport*, 2nd edition. 2001 Gulf Professional Publishing, U.S.A.
- [16] Dresser, A. (1979). *Log Interpretation Charts*. Dresser Industries Inc., Houston, Texas, Page 107.
- [17] Cannon, S. (2018). *Reservoir Modelling: A Practical Guide*. John Wiley and Sons, Inc., 111 River Street, Hoboken, NJ 07030, USA.
- [18] Archie, G.E. (1942). The electrical resistivity log as an aid in determining some reservoir characteristics. *Journal of Petroleum Technology*, 5: 54–62.
- [19] Levorsen, A.I. (1967). *The geology of petroleum*, 2nd edition. Freeman, San Francisco, Page 724.
- [20] Rider, M.H. (1996). *The Geological Interpretation of Well Logs*, 2nd edition. Whittles Publishing, Caithness.